Modupeola and Patricia
Beni-Suef Univ J Basic Appl Sci (2024) 13:87
https://doi.org/10.1186/s43088-024-00542-5

Beni-Suef University Journal of Basic and Applied Sciences

RESEARCH

Open Access

Optimizing the maximum strain of a laser-deposited high-entropy alloy using COMSOL multiphysics

Dada Modupeola[1*] and Popoola Patricia[1]

Abstract

Background Laser metal deposition (LMD) is a widely used additive manufacturing technique for producing complex high entropy alloys with special properties for several applications. The AlCoCrFeNiCu HEAs compositional design has six elements with a configurational entropy of 1.79 R and atomic concentrations between 5 and 35%, so the HEA system is thermodynamically favorable according to Boltzmann's theory, attributed to the core effects. However, the high-entropy alloy has dominant Body-Centered Cubic structures which may be too brittle to be examined in tension experimentally. Preheating the substrate before and during layer deposition could be a potential solution that is currently under development since tensile loading necessitates an understanding of a material's behavior under tension through an analysis of its yield and ultimate tensile strength. A computer-aided design (CAD) solid model was used to generate the near-net dog-bone form of the alloy with moderately complicated geometrical characteristics using laser metal deposition (LMD) technology. This study investigates a straightforward and effective computational model for simulating material properties, using COMSOL Multiphysics 5.4 software for laser-deposited high entropy alloys that are excessively brittle to be tested in tension. The AlCoCrFeNiCu high-entropy alloy "dog bone" test sample was modeled using COMSOL Multiphysics for tensile loading. The first principal stresses and longitudinal strain under axial loading conditions were measured using a three-dimensional (3D) structural mechanics' model.

Results The results showed the ultimate tensile strength is 8.47 N/m^2, attributed to the high entropy effect and the dominant phase structure of the alloy.

Conclusion Numerical models in this paper demonstrate the effect of stresses on the tensile behavior of the AlCoCrFeNiCu high-entropy alloy. The model optimizes the LMD process by analyzing residual stresses and predicting tensile strength, thus, providing insights that show the potential of high entropy alloys for structural integrity in aerospace applications.

Keywords COMSOL multiphysics, High entropy alloys, Additive manufacturing, Tensile

1 Background

In recent years, to reduce weight, increase fuel efficiency, and lower emissions, lightweight materials with high specific strength and stiffness have been required for aerospace applications. This has led to the innovation of alloy materials with improved microstructural and mechanical properties to meet the challenging requirements for aerospace components [1–3]. Alloying has been employed to give materials desirable qualities. It entails mixing a major element with a minor amount of a secondary

*Correspondence:
Dada Modupeola
dadadupeola@gmail.com
[1] Department of Chemical, Metallurgical and Materials Engineering, Tshwane University of Technology, Staatsartillerie Rd, Pretoria West, Pretoria 0183, South Africa

element. To generate novel materials known as high-entropy alloys (HEAs), a new alloying technique that combines many principal elements in optimized concentrations has gained research interest [4, 5]. Although only a small part of the multi-dimensional compositional space has been studied, it is nearly infinite. However, a few high-entropy alloys have already been shown to have amazing qualities that surpass those of conventional alloys. The AlCoCrFeNiCu HEAs compositional design has six elements with a configurational entropy of 1.79 R and atomic concentrations between 5 and 35%, so the high-entropy alloy (HEA) system is thermodynamically favorable. Boltzmann's theory shows the role of entropy on alloys; while, its core effects are one of the factors that denote stability [6–9]. The sluggish diffusion effect contributes to the growth of amorphous structures or monocrystalline structures [10]. The lattice distortion effect dictates the properties of the alloy; while, the high entropy effect contributes to the merging of alloys having compatible elements in a composition and comprising solid solution phases or single phases [11, 12]. The cocktail effect relies on the contribution of each principal element in the composition, resulting in the bulk property of the alloy composition. These core effects improve the electrochemical, tribological, thermal, and mechanical properties of HEA materials, especially. However, most of the AlCoCrFeNiCu high-entropy alloy compositions contain single-structured or predominant Body-Centered Cubic (BCC) phases and/or intermetallic compounds, which may make the alloy brittle and difficult to machine or test for tension, especially via advanced manufacturing techniques [5]. The aerospace industry has a lot of components built via the three-dimensional (3D) additive manufacturing (AM) technique, which builds parts layer by layer and has the potential to generate parts that are stronger, lighter, and better engineered than traditional parts [13, 14]. Additionally, AM technology can produce unique or replacement parts from any location, at any time, and more quickly than previous procedures [15, 16]. However, the high contact area between layers causes worse performance under tension if the part's consecutive layers lack cohesiveness. As with many design methodologies, AM optimization is traditionally thought of as a process parameter optimization, especially when directed toward topology optimization in the generation of the geometry through a computer-aided design (CAD) model [17–19]. To determine the stress–strain mechanism of laser-deposited high-entropy alloy test samples, the amalgams are subjected to tensile testing. In many industries, such as construction, aerospace, automotive, machinery, biomedical implants, and consumer goods, tensile strength is essential. For structural integrity, cables, steel beams, and concrete reinforcement bars are needed in buildings and bridges. For structural integrity, the fuselage and wings of an aircraft need to have extraordinary tensile strength. For safety, airbags and seatbelts must be able to withstand extremely high tensile forces. Using the phase-field method, Li et al. [30] simulated coherent BCC/B2 microstructures in Al–Ni–Co-Fe–Cr HEAs based on BCC using COMSOL. Precipitate morphology was influenced by the lattice misfit and Young's moduli anisotropy difference, as demonstrated by the simulations' results, which were in agreement with the experimental findings. Additionally, the study covered the coarsening behavior of precipitates and offered a method for forecasting composition design and microstructural evolution. FeCoNi(Mn–Si)x HEAs were created by Sahu et al. [31] using mechanical alloying. X-ray diffraction (XRD), Scanning Electron Microscope (SEM), and *Transmission Electron Microscope* (TEM) were used to examine how the Mn and Si content affected the alloy's magnetic behavior and structure. The surface morphology was found to be affected by high Mn and Si content, resulting in a shift from the BCC phase to the Face Centered Cubic (FCC) phase. The magnetic flux density on the transformer core was measured with the finite element method (FEM) and COMSOL Multiphysics software to evaluate the performance of the proposed HEAs. The magnetic flux density on the transformer core was measured with the FEM and COMSOL Multiphysics software to evaluate the performance of the proposed HEAs. For laser cladding AlCrNiTiNb high-entropy alloy (HEA) coatings on titanium alloy (Ti6Al4V) substrates, a three-dimensional FEA model was created by Kayane et al. [32]. Because of its great strength but low hardness, Ti6Al4V is used in the automotive, aerospace, and marine industries. Using a laser cladding technique, the study synthesized AlCrNiTiNb HEA hard coating with an equiatomic ratio. Heat transfer in solids modules was modeled using COMSOL Multiphysics 5.3a, which revealed a dendritic and interdendritic structure in the AlCrNiTiNb alloy coating. Solid solution phases were found to be both ordered and disordered by X-ray diffraction, and intermetallic compounds were absent. The combination of the FCC and BCC solid solution phases greatly enhanced the coating's microhardness. The coating exhibits strong metallurgical bonding and a dendritic and interdendritic structure. The coating has a higher microhardness than the substrate.

In the literature, the microstructure, magnetic flux density, and heat transfer of HEAs have been simulated using COMSOL, with limited studies on the tensile properties of the HEAs fabricated via additive manufacturing. Hence, due to geometrical restrictions and difficulties experienced in building specific dog-bone shapes of alloy samples with brittle dominant BCC structures via

additive manufacturing, computational simulation can be applied as a possible solution to determining the tensile properties of these alloys. The complexity, material properties, validation, computational efficiency, software, and user-friendliness of a proposed tensile loading model for laser-deposited HEAs using COMSOL Multiphysics are taken into account to assess the model's uniqueness and high performance. To improve prediction accuracy, temperature-dependent material properties and the unique composition of HEA were taken into consideration. COMSOL's features were used for a more approachable interface, simpler customization, and wider research community adoption.

There are limited reports in the literature on laser-deposited high entropy alloys available on this subject. In this study, the COMSOL finite element model was used to simulate the mechanical behavior of an AlCoCrFeNiCu high-entropy alloy sample to solve the structural mechanics challenge of the additive manufacturing process. Computational analysis of AlCoCrFeNiCu HEA composition is currently understudied in the literature; hence, this study may aid in the creation of a more successful modeling strategy for HEA systems. From this study, new functionalities within COMSOL Multiphysics for tensile loading simulations, such as user-defined material properties or coupling with other physical phenomena like heat transfer, may also be reviewed and explored for other HEA compositions.

2 Methods

The composition of AlCoCrFeNiCu HEA powder was acquired from F.J. Brodmann & CO., L.L.C, New Orleans, USA. The laser engineering net shaping (LENS) system was used to fabricate the HEA powder on a preheated A301 steel substrate using optimized parameters [20]. The beam diameter of 2 mm, the powder feed rate of 2 rpm, the 50% overlap, and the layer thickness of 0.5 mm were used for the direct energy deposition (DED). The laser power ranges from 1200 to 1600 W, and the scan speed ranges from 8 mm/s to 12 mm/s. The elastic modulus was measured using Anton Paar TTX-NHT^3 Nanoindentation tester. With geometry created in SolidWorks and imported via the COMSOL CAD Import Module, a 3D Solid Mechanics physics model was created using COMSOL Multiphysics 5.4. The AlCoCrFeNiCu HEA dog-bone sample was modeled as a homogenous, linearly elastic component with the dog-bone's left end designated as a fixed constraint boundary. The right-hand side of the dog-bone's sample received point boundary loads in the y direction. Using the solver's default settings, a stationary analysis was carried out on a fine physics-controlled mesh and an analysis with the stationary study was performed using the intended load range of 10 kN–20 kN in the default solver setting.

2.1 Equations

Three equations such as equilibrium balance, a constitutive relation between stress and strain, and a kinematic relation between displacement and strain were needed to model the high-entropy alloy sample. The equilibrium equation, which is Newton's second law in tensor form, is represented in Eq. 1 [23]:

$$\Delta \cdot \sigma + F_v = \rho \ddot{u} \tag{1}$$

where F_v is the force per volume, σ is the stress, ü is the acceleration and ρ is the density. For static analysis, the right side of this equation equals 0. The constitutive equation that links the stress tensor to strain is the generalized Hooke's law stated as Eq. 2 and expanded as Eq. 3 [23]:

$$\sigma = C : \epsilon \tag{2}$$

$$\sigma - \sigma_0 = C : (\epsilon - \epsilon_0 - \epsilon_{\text{inel}}) \tag{3}$$

where the semicolon is the double dot tensor, $\sigma_0 and \epsilon_0$ is the initial stress and strain, respectively. C is the elasticity tensor in fourth order and ϵ_{inel} is the inelastic strain all equal to zero. The elastic tensor is reduced to a 6×6 elastic matrix for isotropic high entropy alloys using Eq. 4 [23]:

$$\begin{bmatrix} 2\mu+\lambda & \lambda & \lambda & 0 & 0 & 0 \\ \lambda & 2\mu+\lambda & \lambda & 0 & 0 & 0 \\ \lambda & \lambda & 2\mu+\lambda & 0 & 0 & 0 \\ 0 & 0 & 0 & \mu & 0 & 0 \\ 0 & 0 & 0 & 0 & \mu & 0 \\ 0 & 0 & 0 & 0 & 0 & \mu \end{bmatrix} \tag{4}$$

where the μ and ℶ are the Lamé constants, υ is the Poisson's ratio and E is the elastic modulus of the AlCoCrFeNiCu high-entropy alloy. Table 1 lists the material properties; while, the kinematic relationship between the strain ϵ and the displacement $\varkappa$ in tensor format are expressed in Eq. 5 [23]:

Table 1 Material Parameters of the AlCoCrFeBiCu High Entropy Alloys used for the Simulation [20]

Name	Value	Unit
Density	7026	kg/m^3
Young's modulus	149	GPa
Poisson's ratio	0.3	1

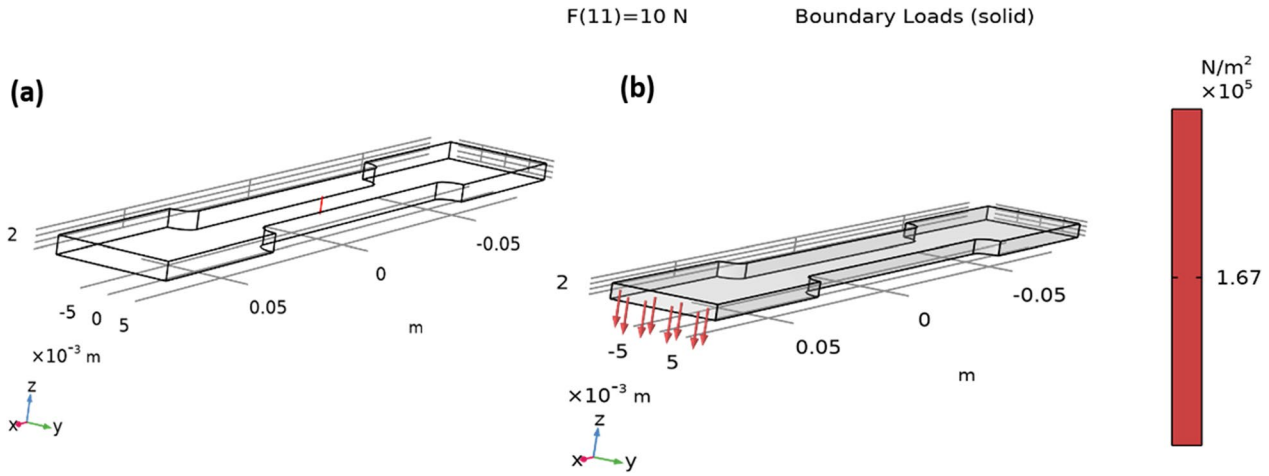

Fig. 1 **a** Geometry **b** Effect of the 10 kN Boundary Load

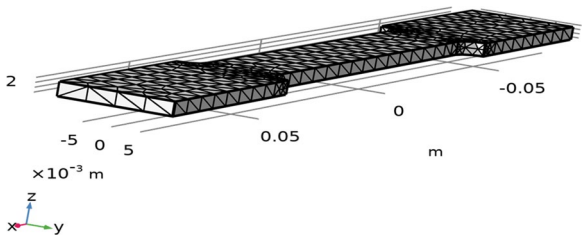

Fig. 2 COMSOL Multiphysics Fine Mesh of the AlCoCrFeNiCu High Entropy Alloy Test Sample

$$\epsilon = \frac{1}{2}\left[\nabla \mu + (\nabla \mu)^T\right] \tag{5}$$

where the ^{T} is the tensor transpose; while, small deformations in a very high order terminology are negligible but the strain reduces to a Cauchy infinitesimal strain tensor ϵ_{ij} shown in Eq. 6 [23]:

$$\epsilon_{ij} = \frac{1}{2}\left[\frac{\delta \mu_j}{\delta x_i} + \frac{\delta \mu_i}{\delta x_j}\right] \tag{6}$$

3 Results

The AlCoCrFeNiCu High-Entropy alloy dog-bone geometry with dimensions in meters is shown in Fig. 1a; the influence of the boundary load of 10 kN is displayed in Fig. 1b.

Using the solver's default settings, a stationary analysis was carried out on a fine physics-controlled mesh in Fig. 2. The displacement magnitude at 2.76 m and the resulting energy per volume or energy density at 2.31×10^7 J/m^3 are represented in Fig. 3a and 3b, respectively. The test region experiences uniform stress, as anticipated. The total displacement is zero because the sample is held in place without any movement [24]. The ratio of the change in volume to the original volume represented as the volumetric strain, is represented

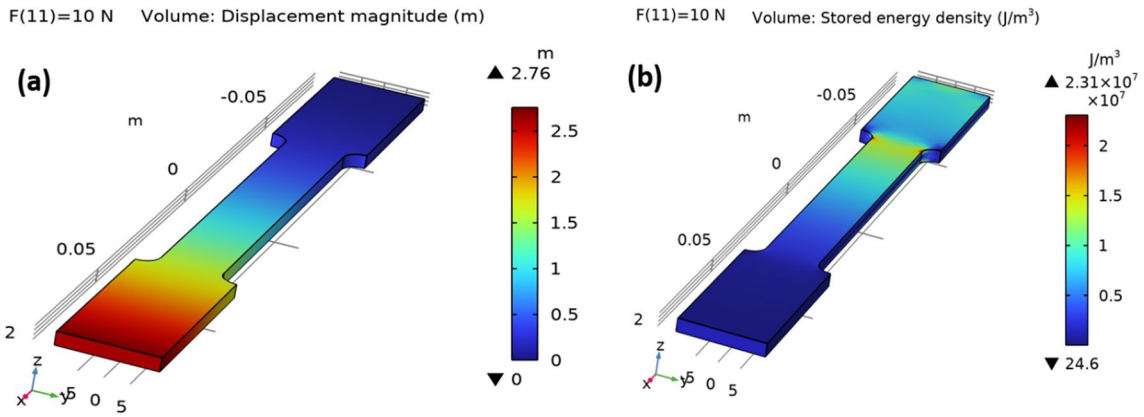

Fig. 3 **a** Displacement Magnitude (m) **b** Stored Energy Density (J/m.^{3})

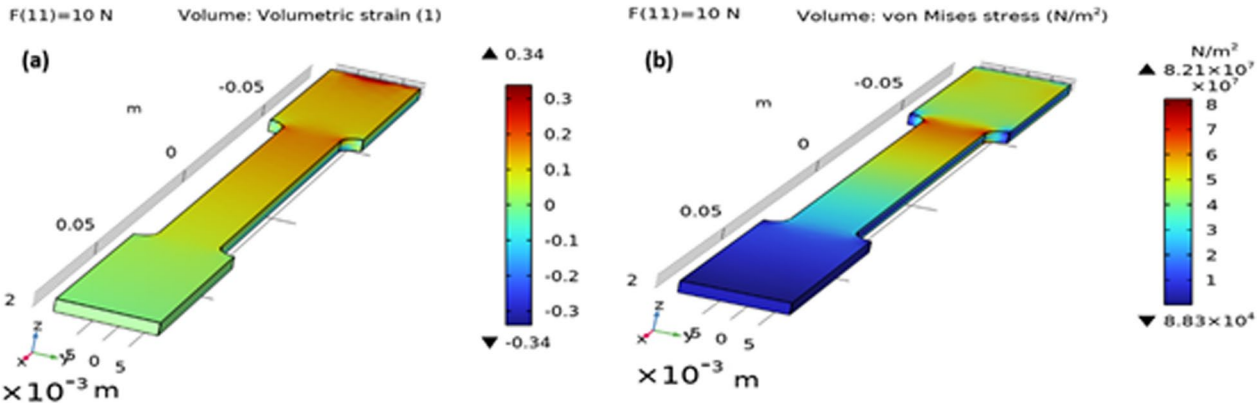

Fig. 4 **a** Volumetric Strain **b** Von Mises Stress

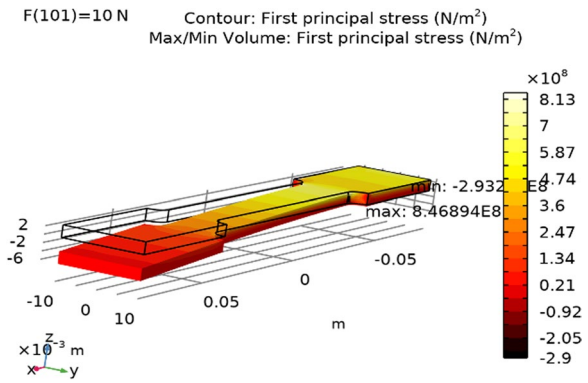

Fig. 5 First and Second Principal Strain Contour Plot for the AlCoCrFeNiCu High Entropy Alloy with A Load of 10 N, Showing the Complexity of Strains near the Sample Grip Ends and the Test Region with a Uniform Center

in Fig. 4a. The Von Mises stress in Fig. 4b at 8.83 N/m^2 shows when the alloy will yield or fracture. Hence, if the value is greater than the yield limit under tension, the alloy is expected to yield [25]. A contour plot of the first and second major strains is shown in Fig. 5.

Temperature dependence of the HEA is relevant because it aids in the prediction of failure mechanisms, residual stresses, and the strength and ductility of the coating. Comprehending these variables aids in guaranteeing that the coating can tolerate anticipated loads, forecasting the progression of residual stresses, and projecting the coating's lifespan and modes of failure.

A probe plot showing the total displacement of the deformed shape of the alloy at a certain load is shown in Fig. 6a, where the correlation efficiency is 1. The measured

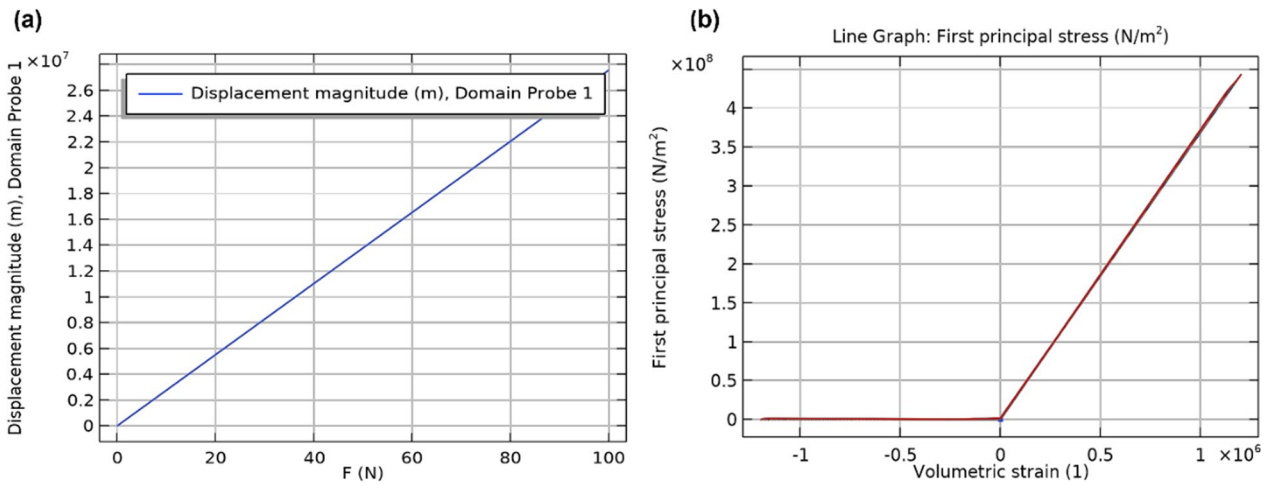

Fig. 6 Line Graph Showing **a** Probe Plot **b** The First Principal Stress (N/m^2) Vs the Volumetric Strain Curve

first principal stress and volumetric strain are shown in Fig. 6b for the sample.

The AlCoCrFeNiCu HEA solid sample in Fig. 7 was accurately weighed to 1.5 g and placed into the sample chamber and the lid was closed shown.

From Table 2, the gas pycnometer determined the volume at 0.2135 cm^3 and the density was given as 7.026 g/cm^3. Which is less than stainless steels, Inconel 738LC and other high temperature materials with densities between 7.3 g/cm^3 and 9 g/cm^3 [21, 22].

4 Discussion

The modulus of the AlCoCrFeNiCu High-Entropy alloy sample was derived via Nanoindentation tests in previous studies [20]. The density measurements using an Anton Paar Single Station Gas Pycnometer for True Density; Ultrapyc 1200e were made after laser metal deposition assisted with preheat (LMDAP) was used. Then helium was purged through the chamber for 9 or more minutes to remove moisture and air from the chamber. The expansion and sample chambers were closed for helium to be introduced again into the sample chamber at a preset pressure of ~ 17 Pa. The system used about 250 to 300 s to stabilize before recording the chamber pressure, P_1, then the valve was opened again to let out the pressurized helium from the sample chamber to flow into the expansion chamber to create another pressure P_2 in about 300 s. The volume of the sample is calculated from Eq. 7 [26].

$$V_{\text{sample}} = V_{\text{Cell}} + \frac{V_{\text{exp}}}{\frac{P_1 - P_a}{P_2 - P_a} - 1} \tag{7}$$

Fig. 7 Laser-Deposited AlCoCrFeNiCu High Entropy Alloy Sample

The sample cell volume is V_{Cell}, the sample volume is V_{sample}, the expansion cell volume is V_{exp}, and the ambient pressure is P_a, respectively. The density is calculated from the measured volume and the sample weight. The characterization of the density measurements of the as-built AlCoCrFeNiCu HEAs was based on pressure–volume relationships using Boyle's and Mariotte's law. The elastic modulus and density that were extracted through experimental analysis demonstrated that this simulated method via COMSOL is capable of measuring material properties with accuracy for any high-entropy alloy sample, which was predicted by the model results.

A fixed constraint boundary was applied to one end of the sample, which restricted the degree of freedom over all the assigned objects. This constraint models the geometry connected to a rigid body or a boundary load. Stress concentrations are expected to occur in regions very close to the assigned face of load application [27]. Hence, a mesh was applied to smoothen the stress gradients and extract the exact stress values at different concentration points. While a boundary load of 10 kN was applied to the other end using a parametric sweep while keeping the alloy linearly elastic. The maximum ultimate tensile strength of the model was approximately given as 8.46 N/m^2, which is the maximum stress the AlCoCrfeNiCu HEA alloy can withstand before failure. Typically, an alloy with a high ultimate tensile strength (UTS) can withstand a lot of force per unit area. This is a weak and potentially broken HEA due to low stress, possibly due to brittleness [28]. Energy loss was not accounted for, which is one of the limitations of this study because the temperature distribution, microstructure, and mechanical properties of the laser-deposited HEA may have been enhanced by accounting for energy loss in the model. This could lead to larger grain sizes and residual stresses, which could affect the performance of the coating under load. Hence, further studies are recommended because gaining insight into the reasons behind this particular composition's low strength could help to enhance HEA production techniques and comprehend how element ratios impact mechanical properties.

Nonetheless, this work investigates the under researched topic of using computational analysis of AlCoCrFeNiCu HEA composition in literature using COMSOL Multiphysics. From the contour map, it was obvious that there was a uniform center test region, inches long, where strain gages may be installed for precise strain measurements, despite the complicated local

Table 2 Density Measurements and Processing Parameters for the As-Built AlCoCrFeNiCu High Entropy Alloy Sample

High entropy alloys	Laser power (W) (J/s)	Scan speed (V) (mm/s)	Mass of sample (g)	Volume (cm^3)	Density (g/cm^3)	Temperature (°C)
AlCoCrFeNiCu	1400	12	1.5	0.2082	7.204	25.935

stresses near the grips (ends). The measured strain was linear under the full-applied load range of 10 kN showing the deformation progression of the AlCoCrFeNiCu HEA. The strain curve showed the tendency of the AlCoCrFeNiCu HEA to deform when uniformly loaded in all directions. The first principal stress expressed the maximum tensile stress induced by boundary load conditions; while, the volumetric strain showed the ratio of the change in the volume of the alloy to the original volume when an external load was applied [29].

5 Conclusion

Despite its simplicity, the AlCoCrFeNiCu high-entropy alloy sample's maximum tensile stress was estimated using COMSOL Multiphysics. The model was useful in studying the stress concentrations between the grab regions at the test sample ends. With a tensile strength of 0.847 Pa, the weak HEA is unlikely to support a large load and could fracture at low stress at its current state and may be suitable for lightweight fillers or dampening vibration applications. The high sensitivity correlates with the brittleness of the alloy which limits its application However, optimizing the alloy composition, applying heat treatment or severe plastic deformation may enhance the tensile properties of this alloy. Hence, the computational model made it possible to visualize phenomena like Saint–Venant's principle in high entropy alloys, a topic that is now of research interest.

Abbreviations

BCC	Body-Centered Cubic
CAD	Computer-aided design
LMD	Laser metal deposition
3D	Three dimensional
HEAs	High-entropy alloys
AM	Additive manufacturing
FCC	Face centered cubic phase
FEM	Finite element method
LENS	Laser engineering net shaping
DED	Direct energy deposition
LMDAP	Laser metal deposition assisted with preheat
UTS	Ultimate tensile strength

Acknowledgements
The authors appreciate the Laser Enabled Manufacturing Resource Group at the Council for Scientific and Industrial Research CSIR, and the Surface Engineering Research Laboratory (SERL) for their Technical Support.

Author contributions
MD involved in conceptualization, data curation, writing and editing and reviewing of draft. PP involved in conceptualization, supervision, data curation, and editing and reviewing of draft.

Funding
Not applicable.

Availability of data and materials
Not applicable.

Declarations

Ethics approval and consent to participate.
Not applicable.

Consent for publication.
Not applicable.

Competing interests
All authors declare that they have no competing interests.

Received: 25 March 2024 Accepted: 13 August 2024
Published online: 05 September 2024

References

1. Mangalgiri PD (1999) Composite materials for aerospace applications. Bull Mater Sci 22:657–664
2. Bhat A, Budholiya S, Aravind Raj S, Sultan MTH, Hui D, Md Shah AU, Safri SNA (2021) Review on nanocomposites based on aerospace applications. Nanotechnol Rev 10(1):237–253
3. Tepylo N, Huang X, Patnaik PC (2019) Laser-based additive manufacturing technologies for aerospace applications. Adv Eng Mater 21(11):1900617
4. Moghaddam AO, Shaburova NA, Samodurova MN, Abdollahzadeh A, Trofimov EA (2021) Additive manufacturing of high entropy alloys: a practical review. J Mater Sci Technol 77:131–162
5. Chen J, Zhou X, Wang W, Liu B, Lv Y, Yang W, Xu D, Liu Y (2018) A review on fundamental of high entropy alloys with promising high–temperature properties. J Alloy Compd 760:15–30
6. Zhou YK, Kang JJ, Zhang J, Fu ZQ, Zhu LN, She DS (2022) Effect of vacuum heat treatment on microstructure and mechanical properties of HVOF sprayed AlCoCrFeNiCu high-entropy alloy coating. Mater Lett 323:132551
7. Yu Y, Wang J, Yang J, Qiao Z, Duan H, Li J, Li J, Liu W (2019) Corrosive and tribological behaviors of AlCoCrFeNi-M high entropy alloys under 90 wt.% H_2O_2 solution. Tribol Int 131:24–32
8. Miracle DB (2017) High-entropy alloys: a current evaluation of founding ideas and core effects and exploring "nonlinear alloys." Jom 69(11):2130–2136
9. Mehta A, Sohn YH (2021) Fundamental core effects in transition metal high-entropy alloys:"High-entropy" and "sluggish diffusion" effects. Diffus Found 29:75–93
10. Mehta A, Sohn Y (2020) High entropy and sluggish diffusion "Core" effects in senary FCC Al–Co–Cr–Fe–Ni–Mn alloys. ACS Comb Sci 22(12):757–767
11. Lee C, Chou Y, Kim G, Gao MC, An K, Brechtl J, Zhang C, Chen W, Poplawsky JD, Song G, Ren Y (2020) Lattice-distortion-enhanced yield strength in a refractory high-entropy alloy. Adv Mater 32(49):2004029
12. Song H, Tian F, Hu QM, Vitos L, Wang Y, Shen J, Chen N (2017) Local lattice distortion in high-entropy alloys. Phys Rev Mater 1(2):023404
13 Wong KV, Hernandez A (2012) A review of additive manufacturing. Int Sch Res Not 2012(1):208760
14. Frazier WE (2014) Metal additive manufacturing: a review. J Mater Eng Perform 23:1917–1928
15. Dilberoglu UM, Gharehpapagh B, Yaman U, Dolen M (2017) The role of additive manufacturing in the era of industry 4.0. Procedia Manuf 11:545–554
16 Bandyopadhyay A, Bose S (eds) (2019) Additive manufacturing. CRC Press, Boca Raton
17 Medeiros e Sa A, Mello VM, Rodriguez Echavarria K, Covill D (2015) Adaptive voids: primal and dual adaptive cellular structures for additive manufacturing. Vis Comput 31:799–808
18. Javaid M, Haleem A (2019) Current status and challenges of Additive manufacturing in orthopaedics: an overview. J Clin Orthop Trauma 10(2):380–386
19. Altıparmak SC, Yardley VA, Shi Z, Lin J (2021) Challenges in additive manufacturing of high-strength aluminium alloys and current developments in hybrid additive manufacturing. Int J Lightweight Mater Manuf 4(2):246–261

20. Dada M, Popoola P, Mathe N, Adeosun S, Pityana S (2021) Investigating the elastic modulus and hardness properties of a high entropy alloy coating using nanoindentation. Int J Lightweight Mater Manuf 4(3):339–345
21 Ogunbiyi OF, Sadiku ER, Jamiru T, Adesina OT, Beneke LW (2019) Spark plasma sintering of Inconel 738LC: densification and microstructural characteristics. Mater Res Express 6(10):1065g8
22. Perrut M, Caron P, Thomas M, Couret A (2018) High temperature materials for aerospace applications: Ni-based superalloys and γ-TiAl alloys. C R Phys 19(8):657–671
23. Marchidan, A., Sullivan, T.N. and Palladino, J.L., 2012, October. Load cell design using comsol multiphysics. In *Proceedings of the 2012 COMSOL Conference*. Boston.
24. Simmons RM, Finer JT, Chu S, Spudich JA (1996) Quantitative measurements of force and displacement using an optical trap. Biophys J 70(4):1813–1822
25. Wang YZ, Li GQ, Wang YB, Lyu YF (2021) Simplified method to identify full von Mises stress-strain curve of structural metals. J Constr Steel Res 181:106624
26. Ye Z, Wang Y, Wen Q, Liu Y, Liu C, Xiong X (2023) Effects of density and heat treatment of C/C preforms on microstructure and mechanical properties of C/C–SiC composites. Int J Appl Ceram Technol 20(1):112–124
27. Ahmadi H, Lotfollahi-Yaghin MA, Yong-Bo S, Aminfar MH (2012) Parametric study and formulation of outer-brace geometric stress concentration factors in internally ring-stiffened tubular KT-joints of offshore structures. Appl Ocean Res 38:74–91
28. Han SZ, Choi EA, Lim SH, Kim S, Lee J (2021) Alloy design strategies to increase strength and its trade-offs together. Prog Mater Sci 117:100720
29. Veiga C, Davim JP, Loureiro AJR (2012) Properties and applications of titanium alloys: a brief review. Rev Adv Mater Sci 32(2):133–148
30. Li JL, Li Z, Wang Q, Dong C, Liaw PK (2020) Phase-field simulation of coherent BCC/B2 microstructures in high entropy alloys. Acta Mater 197:10–19
31 Sahu P, Solanki S, Dewangan S, Kumar V (2019) Microstructure and magnetic behavior of FeCoNi (Mn–Si) x (x= 0.5, 0.75, 1.0) high-entropy alloys. J Mater Res 34(5):829–840
32. Kanyane LR, Lepele P, Malatji N, Shongwe MB (2024) 3D finite element analysis and experimental correlations of laser synthesized AlCrNiTiNb high entropy alloy coating. Mater Today Commun 38:107686

Publisher's Note